ELSEVIER

Journal of Alloys and Compounds 311 (2000) 169–180

Journal of ALLOYS AND COMPOUNDS

www.elsevier.com/locate/jallcom

Synthesis and characterization of a novel platinum molybdenum sulfide containing the Mo_6S_8 cluster

Thomas J. Paskach[a,c], Shane J. Hilsenbeck[a,b,c], R. Kirk Thompson[a,c], Robert E. McCarley[b,c], Glenn L. Schrader[a,c,*]

[a]*Department of Chemical Engineering, Ames, IA 50011, USA*
[b]*Department of Chemistry, Ames, IA 50011, USA*
[c]*Ames Laboratory-USDOE, Iowa State University, Ames, IA 50011, USA*

Received 7 April 2000; received in revised form 23 June 2000; accepted 26 June 2000

Abstract

Our previously discovered, low-temperature route for the preparation of ternary molybdenum sulfide cluster compounds containing the Mo_6S_8 structure has been used to synthesize a new Pt (PtMoS) material. Ion-exchange of amorphous NaMoS with $[Pt(NH_3)_4]Cl_2$ led to incorporation of the $[Pt(NH_3)_4]^{2+}$ cation yielding $[Pt(NH_3)_4](Mo_6S_8)S{\cdot}x(H_2O/MeOH)$, as confirmed by infrared and X-ray photoelectron spectroscopic (XPS) characterization. XPS indicated that this new platinum material had the reduced molybdenum oxidation state characteristic of ternary molybdenum sulfides containing the Mo_6S_8 structural unit. The surface area of the new PtMoS material was as high as 135 m^2/g. Attempts to convert the PtMoS material to a crystalline Chevrel phase $PtMo_6S_8$ by H_2 reduction at elevated temperatures were unsuccessful. However, H_2 treatment at 400°C provided material retaining the Mo_6S_8 cluster, probably as amorphous $Pt(Mo_6S_8)S$. The latter material is a very active hydrodesulfurization (HDS) catalyst, with much higher activity compared to other more stable compounds containing the Mo_6S_8 cluster unit. © 2000 Elsevier Science S.A. All rights reserved.

Keywords: Metal sulfide clusters; Molybdenum cluster catalysts; Hydrodesulfurization

1. Introduction

For many years, reduced ternary molybdenum chalcogenides have generated special attention because of their interesting structures and physical or chemical properties. Among these, the Chevrel phases [1], $M_xMo_6Q_8$ (with M either a main group, transition or lanthanide metallic element and Q=S, Se or Te), have attracted the most attention. The common structural motif in these compounds [2] is the three-dimensional cross-linking of Mo_6Q_8 cluster units (Fig. 1) by sharing Q atoms, as indicated in the formula $M_x(Mo_6Q_2Q_{6/2})Q_{6/2}$. The ternary metal atoms, M, reside in interstitial sites created by this network and transfer *n* electrons to the framework as in $M_x^{n+}(Mo_6Q_8^{xn-})$ [3,4]. Up to four electrons per Mo_6Q_8 unit may be transferred [5,6] so *xn* ranges from 1 to 4. Generally, frameworks with four transferred electrons (24 metal–metal bonding electrons per Mo_6Q_8 unit) are semiconducting while those with $xn<4$ are metallic and often superconducting [2,7,8]. The variable valence of the Mo_6Q_8 cluster units is important to both the superconducting and catalytic properties of these compounds. The members of the family $LnMo_6S_8$ (with Ln=La to Lu) have been characterized as excellent hydrodesulfurization (HDS) catalysts for removal of organosulfur compounds found in petroleum [9–13].

Synthesis of stable phases $M_xMo_6Q_8$ generally can be achieved by direct combination of the elements, at temperatures typically in the range 900–1300°C. Metastable phases such as $HgMo_6S_8$ [14], $TlMo_6S_8$ [15], and others must be obtained by indirect methods, such as electrochemical [16] or direct insertion of M into the binary Mo_6S_8 [17]. The latter is itself a metastable phase obtained by demetalation of $NiMo_6S_8$ [17] or $Cu_2Mo_6S_8$ [14,15]. Among the ions of metallic elements M^{n+} that have not yet been incorporated into the sulfide phases $M_xMo_6S_8$ are the group VIII–X members Ru, Rh, Pd, Ru, Ir and Pt. In the present paper, as a step towards the preparation of the

*Corresponding author. Tel.: +1-515-294-0519; fax: +1-515-294-2689.

E-mail address: schrader@iastate.edu (G.L. Schrader).

0925-8388/00/$ – see front matter © 2000 Elsevier Science S.A. All rights reserved.
PII: S0925-8388(00)01107-5

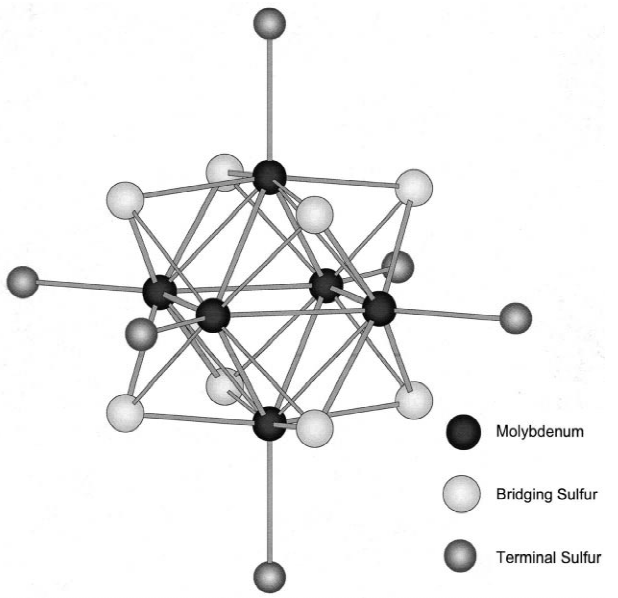

Fig. 1. Structure of the Mo_6S_8 hexanuclear cluster unit formed by a molybdenum octahedron and eight triply bridging sulfur atoms capping each face. Six terminal positions are located at the vertices of the octahedron and are occupied by either organic ligands or sulfur atoms.

latter phases, we show that a platinum-containing derivative, $[Pt(NH_3)_4]Mo_6S_9(H_2O)_m$, can be prepared by ion exchange of $[Pt(NH_3)_4]^{2+}$ with amorphous $Na_2Mo_6S_9$ [18].

2. Experimental

2.1. Materials

Since the reagents and products have been generally found to be air sensitive, all manipulations were performed using an inert-atmosphere drybox, a high-vacuum manifold, and Schlenk equipment, unless otherwise stated. High yields of amorphous ternary sodium molybdenum sulfide, $Na_2(Mo_6S_8)S{\cdot}y$MeOH (y=4–5) (denoted as NaMoS[MeOH][1] were prepared by the reaction of Mo_6Cl_{12} with NaSH and NaOEt in refluxing *n*-BuOH followed by MeOH washing to remove the NaCl by-product [18]. Solvents were degassed by boiling for 5 min followed by immediate isolation. Methanol and butanol were also dried prior to use with a 4 Å Molecular Sieve. UHP (zero) nitrogen and zero hydrogen were used for temperature-programmed desorption/temperature-programmed reduction (TPD/TPR), H_2 treatment, and HDS studies. Thiophene (99+% purity) was supplied by Aldrich and used as received.

2.2. Analytical

Molybdenum was determined gravimetrically as the 8-hydroxyquinolate [19]. Chlorine was analyzed by potentiometric titration with a standardized silver nitrate solution. Quantitative elemental analyses for Pt, Mo, and S were performed with an ARL SEMQ microprobe. The instrument was equipped with wavelength dispersive spectroscopy detectors and was operated at 10 kV and 25 nA. Powder samples were loaded in a dry box on double-stick carbon discs and placed in a sealed sample holder designed for air-sensitive samples. Peak profiles and backgrounds were determined for standards immediately before the analyses. At least ten regions for each sample were examined, and the compositional data were averaged.

Additional quantitative elemental analysis for Pt, Mo, and S were performed by inductively coupled plasma (ICP) spectroscopy. Solutions were prepared by dissolving samples with hot aqua regia (50:50 concentrated HCl and HNO_3) followed by dilution to standard volume with deionized water. Analyses for Na were performed on the same solutions by atomic absorption spectroscopy (AAS). Solid samples were first degassed under vacuum at 150°C overnight to remove about 5 wt% volatile solvent.

2.3. Preparation of the ternary platinum molybdenum sulfide

Three methods were used to synthesize the ternary platinum molybdenum sulfides PtMoS[H_2O], PtMoS-[MeOH], and PtMoS[5% H_2O]. NaMoS[MeOH] (1.00 g) and $[Pt(NH_3)_4]Cl_2{\cdot}H_2O$ (0.34 g) were placed into a 100-ml Schlenk reaction flask in the drybox. Three variations in the preparation procedure involved addition of different solvents: (1) 50 ml of degassed H_2O, (2) 50 ml of dried, degassed MeOH, or (3) 57 ml of degassed MeOH and 3 ml of deoxygenated water. After the mixture was stirred at room temperature for 1–2 days, a black solid and faintly colored solution were obtained. The black solid was then filtered from the solution. For the preparations involving MeOH, the solid was rinsed three–six times with 20–30 ml aliquots of dried, deoxygenated MeOH. All PtMoS samples were dried under vacuum overnight and stored in the drybox.

2.4. Characterization methods

Materials were characterized by X-ray photoelectron spectroscopy (XPS), infrared spectroscopy (FTIR), laser Raman spectroscopy (LRS), and X-ray diffraction (XRD). XPS data were obtained with a Physical Electronics Industries 5500 multitechnique surface analysis system

[1]Since the composition of these materials depends on the stoichiometry of the reaction and solvent utilized, we indicate the formula of $Na_2(Mo_6S_8)S{\cdot}4$MeOH prepared in MeOH as NaMoS[MeOH], PtMoS[H_2O] for $Pt(NH_3)_4(Mo_6S_8){\cdot}4H_2O$ prepared in water, etc. PtMoS[5% H_2O] refers to PtMoS prepared in a 5% water/95% MeOH mixture.

using a monochromatic MgK_α source; binding energies were calibrated with adventitious C (C 1s=284.6 eV). Infrared spectra (4000–200 cm^{-1}) were recorded in Nujol mulls with a Bomem MB-102 Fourier transform infrared spectrometer equipped with CsI optics. Laser Raman spectra were obtained in backscattering mode with a Kaiser Holospec f/1.8 spectrometer. A Coherent 532-50 diode-pumped solid state laser was used as the source (532 nm, 50 mW at the source) and a Princeton Instruments CCD (1100×330) was used with WINSPEC software for data acquisition and processing. XRD data were collected only on air-stable samples, in air using a Scintag 2000 θ-θ powder XRD instrument with CuK_α radiation at 45 kV bias and 30-mA emission current.

The surface areas of the compounds were determined according to the BET method using a Micromeritics ASAP 2010 instrument. N_2 at 77.35 K was the adsorbate.

2.5. H_2 treatment and temperature-programmed desorption/reduction

For H_2 treatment, PtMoS powder was placed in an alumina boat inside a quartz tube and heated to the desired temperature (200–1000°C) in a flow of pure H_2; this temperature was maintained for 2–4 h. After cooling under this flow, the product was stored in an inert-atmosphere drybox.

TPD studies were performed by heating 250-mg samples to 800°C (10°C/min) in a flow of pure N_2 (10 sccm). Temperatures were controlled using an Omega 2010 programmable temperature controller.

Temperature-programmed reduction (TPR) studies were conducted using a 6-mm O.D. 4-mm I.D. quartz reactor. TPR experiments were performed after samples had undergone TPD to 800°C. A mixture of 1 sccm H_2 and 10 sccm N_2 was used in these studies, and a heating rate of 10°C/min achieved an acceptable resolution and signal-to-noise ratio. During TPR, the effluent passed through Teflon-lined stainless steel tubing to a Varian 3600CX gas chromatograph having a thermal conductivity detector and to a UTI 100C residual gas analyzer. Product separation by gas chromatography was achieved with an eight foot glass-lined Hayesep-Q column.

2.6. Catalytic studies for thiophene HDS

HDS studies were performed at atmospheric pressure using thiophene as the model organosulfur compound. The reactor system used in these experiments has been described previously [20]. A 0.25-inch stainless steel reactor was loaded with 150 mg of catalyst in the drybox and heated to 400°C in a mixed He (19 sccm) and H_2 (22 sccm) gas flow. At 400°C, this flow was replaced by a continuous flow of 2% thiophene in H_2 (22 sccm). Gas chromatograph analyses were performed after 20 min and after each hour for the 10-h reaction study. After the HDS measurements, the catalyst was cooled under flowing He and stored in the drybox.

3. Results and discussion

3.1. Stoichiometry

The platinum ammine salt used for the ion exchange reaction, $[Pt(NH_3)_4]Cl_2 \cdot H_2O$, was readily soluble in water and resulted in the formation of PtMoS[H_2O] upon reaction with NaMoS. Addition of a small amount of water (5%) to MeOH also achieved complete dissolution of $[Pt(NH_3)_4]Cl_2 \cdot H_2O$ during the ion exchange reaction to form PtMoS[5% H_2O]. In contrast, attempts to prepare the ternary molybdenum sulfide in pure methanol encountered difficulties due to the limited solubility of the platinum ammine salt; platinum ammine salt remained in the final product unless extensively washed with MeOH. This problem was obvious after materials had been dried and washed for a second time. XRD characterization of the (dried) filtrate from this washing revealed $[Pt(NH_3)_4]Cl_2 \cdot H_2O$ and NaCl.

Stoichiometries (ignoring inclusion of solvent molecules) determined from microprobe analysis and Mo gravimetric analysis were $Pt_{0.96}Mo_6S_{8.95}$ for PtMoS[H_2O] and $Pt_{1.05}Mo_6S_{9.07}$ for PtMoS[5% H_2O]. Analytical data from ICP and AAS (Table 1) indicated that the stoichiometry was $Pt_{0.86}Na_{0.076}Mo_6S_{8.3}$ for the first material and $Pt_{0.80}Na_{0.071}Mo_6S_{8.1}$ for the second material. A third

Table 1
Analytical results by ICP and AAS for PtMoS prepared by various ion exchange reactions

	Pt wt%	Mo wt%	S wt%	Na wt%	Pt/(Mo_6) mol/mol	S/(Mo_6) mol/mol	Na/(Mo_6) mol/mol
Measured (volatile-free basis)							
$Pt(NH_3)_4Mo_6S_9 \cdot [H_2O]$	13	46	21	0.14	0.85	8.3	0.075
$Pt(NH_3)_4Mo_6S_9 \cdot [Me_2OH]$	14	46	21	0.13	0.93	8.1	0.072
$Pt(NH_3)_4Mo_6S_9 \cdot [MeOH]$	13	47	22	0.13	0.80	8.2	0.071
Calculated (volatile-free basis)							
$Pt(NH_3)_4Mo_6S_9 \cdot 4[H_2O]$	16	48	24	0	1	9	0
$Pt(NH_3)_4Mo_6S_9 \cdot 4[Me_2OH]$	16	46	23	0	1	9	0

sample synthesized in pure MeOH had the composition $Pt_{0.93}Na_{0.072}Mo_6S_{8.1}$ by ICP/AAS.

Although $[Pt(NH_3)_4]Cl_2 \cdot H_2O$ is only sparingly soluble in MeOH, the ion exchange reaction performed in pure MeOH apparently went to the same degree of completion as with 5% H_2O or pure H_2O. Repeated rinsing with MeOH after the ion exchange completely removed the unreacted $Pt(NH_3)_4Cl_2 \cdot H_2O$ salt. However, removal of Na from the material by the simple stoichiometric ion exchange procedure in any of the three methods was not quite complete. Even with 50% excess Pt salt for the ion exchange reaction, it was still not possible to remove all of the Na.

Sulfur analysis by ICP indicated a lower sulfur stoichiometry than the microprobe data. The results could be systematically low. However, our previous work has demonstrated that oxygen can substitute for sulfur in similarly prepared materials. Fitting of EXAFS results for $SnMo_6S_8$ materials also prepared by the ion exchange method required the inclusion of oxygen, and the stoichiometry was formulated as $SnMo_6O_{0.6}S_{7.4}$ [21].

3.2. Surface area

Surface areas (Table 2) were widely variable but strongly depended on the surface area of the NaMoS starting material. The structure of the material apparently did not change significantly during ion exchange; movement of ions appeared to be possible without significant physical modification of the samples. However, addition of water to the solvent during ion exchange lowered the surface area of the final product. MeOH present within the solvation sphere of the $[Pt(NH_3)_4]^{2+}$ ions and within the pores may have stabilized smaller pores that contribute significantly to the surface area of materials by this technique [22]. Synthesis of the NaMoS starting material in boiling water rather than boiling BuOH typically produced lower surface area materials [23].

As-prepared materials were extremely air sensitive, and even very slight air contamination or exposure significantly reduced the surface area. Samples treated in H_2 at high temperature also had significantly lower surface areas, presumably due to the collapse of smaller pores and sintering.

Table 2
Surface areas by BET (m^2/g) for two different NaMoS starting materials and the PtMoS materials prepared from them by various ion exchange reactions. The surface area of the PtMoS depends largely on the surface area of the NaMoS starting material

	Preparation A	Preparation B
$Na_2Mo_6S_9 \cdot [MeOH]$	39	95
$Pt(NH_3)_4Mo_6S_9 \cdot [H_2O]$	14	55
$Pt(NH_3)_4Mo_6S_9 \cdot [5\% H_2O]$	39	84–87

3.3. Characterization

XPS spectra for Mo and Pt for materials prepared by ion exchange reaction in a 5% H_2O MeOH solution and in pure water are shown in Figs. 2 and 3, respectively. For both synthesis methods, the Mo 3d region typically exhibited Mo peaks having binding energies (Mo $3d_{5/2}$ = 228.1 eV) consistent with that characteristic of the cluster, with a very small amount of surface oxide (probably MoO_3) observed occasionally at higher binding energies. Although Mo metal has nearly the same binding energy as that of Mo_6S_8 clusters, the FTIR and XPS data together clearly indicate that the PtMoS materials contain the cluster units. Fitting of the Pt 4f region showed the presence of only a single species having a binding energy shifted 0.3 eV higher than that for Pt metal (71.2, 74.5 eV).

FTIR spectra for $PtMoS[H_2O]$ and $[Pt(NH_3)_4]Cl_2 \cdot H_2O$ are shown in Fig. 4. Peaks were observed in both spectra at 1558, 1542, 1340, 1325, 889, and 844 cm^{-1} due to various N–H vibrational modes for the $[Pt(NH_3)_4]^{2+}$ salt. The similarity of the spectra provided evidence that the tetraammine cation was present in the compound. The peak at 383 cm^{-1} was assigned to the Mo–S stretching mode characteristic of Mo_6S_8 cluster units [18,21]. Laser Raman spectroscopy did not reveal formation of MoS_2 for the as-prepared material.

3.4. Hydrogen treatment

High-temperature treatment of PtMoS in a flow of pure H_2 for 2 h at 600, 700, 800, 900, and 1000°C was performed in an effort to produce the crystalline Pt Chevrel phase. XRD results (Fig. 5) indicated that below about 900°C, a largely amorphous or at least a very poorly crystalline material was present. At higher temperatures, however, reflections for Mo and a Pt–Mo alloy became apparent, as well as reflections for an unidentified intermediate phase. At 1000°C, the only major reflections observable were due to Mo metal and a Pt–Mo compound, Pt_3Mo_2, probably existing as a solid solution containing excess Mo. By contrast, for experiments where excess Pt was used in the ion exchange or where the product was not washed sufficiently to remove excess Pt salt, XRD results indicated that the high-temperature treatment produced only Pt and Mo metal. For some samples, reflections characteristic of a crystalline hexagonal Chevrel phase were observed at low intensity. In these cases, conversion to the ternary sodium Chevrel phase, due to residual sodium in the starting material was evidently responsible for these reflections.

LRS was performed on the treated samples in order to detect MoS_2. Although none was detected for the as-prepared material, very small peaks characteristic of MoS_2 (383, 404 cm^{-1}) did appear for the 400–600°C treated materials. Comparison of the size of the observed peaks with those of mechanical mixtures of MoS_2 and NaMoS

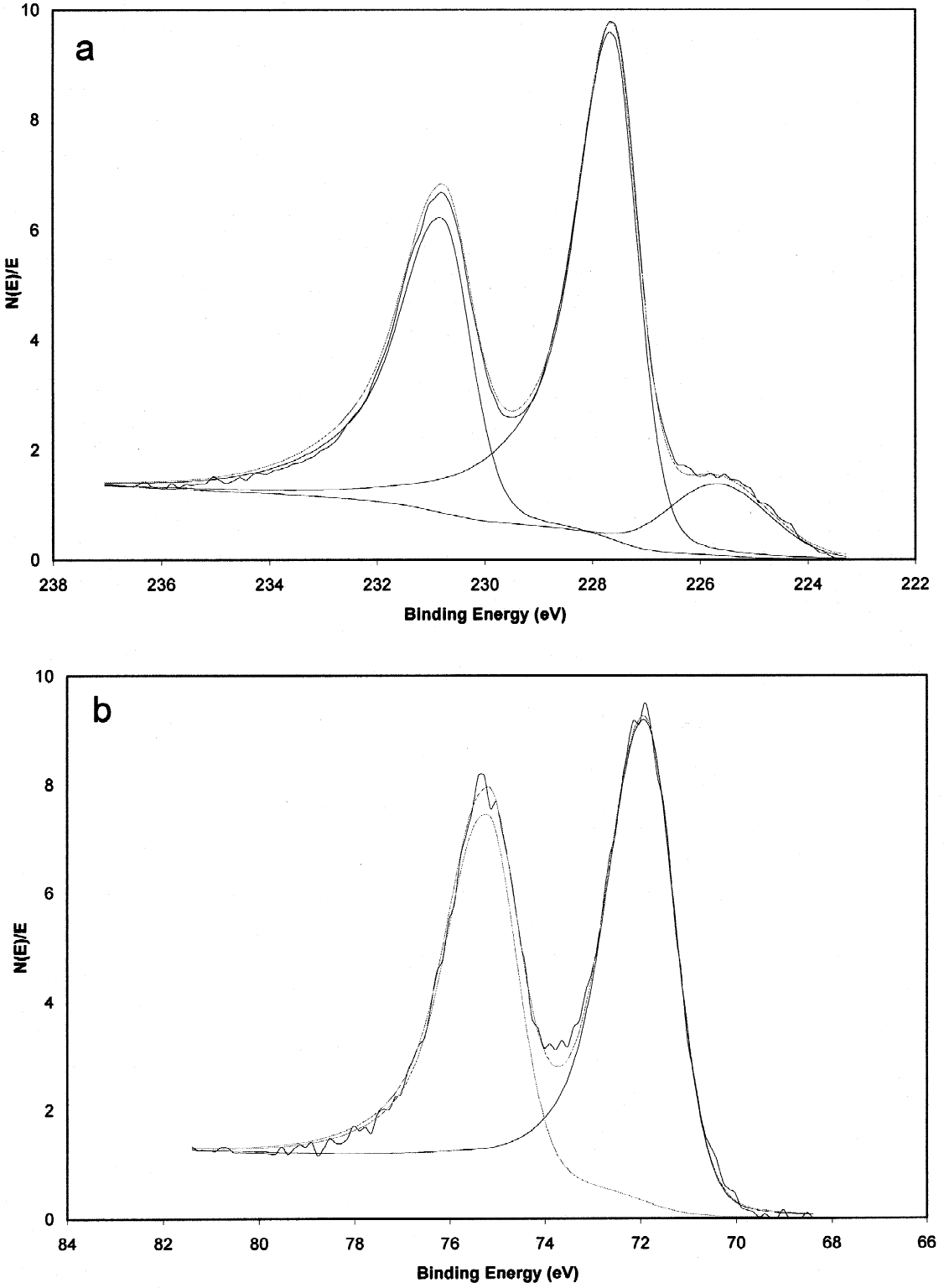

Fig. 2. X-ray photoelectron spectra for PtMoS[5% H_2O] synthesized in a 5% H_2O MeOH solution: (a) Mo 3d and (b) Pt 4f regions. Corrected Mo 3d binding energies are consistent with the Mo_6S_8 cluster unit (228.1 eV) in (a). The broad band observed at the lower binding energy side of the Mo 3d doublets arises from the sulfur 2s peak. Only one type of Pt is detected in (b).

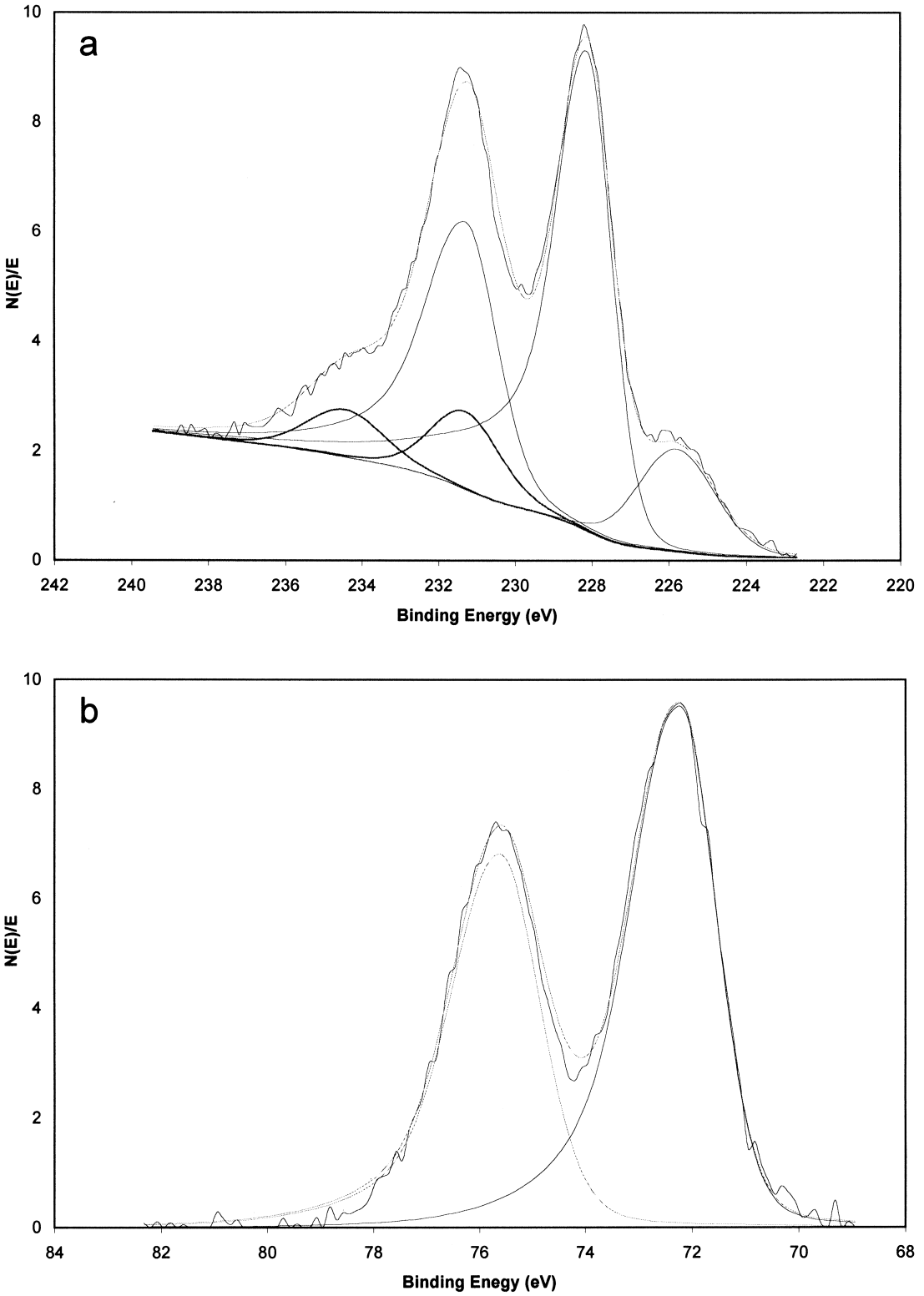

Fig. 3. X-ray photoelectron spectra for PtMoS[H_2O] synthesized in pure water: (a) Mo 3d and (b) Pt 4f regions. Corrected Mo 3d binding energies are consistent with the Mo_6S_8 cluster unit (228.1 eV) and a small amount of surface MoO_3. The broad band observed at the lower binding energy side of the Mo 3d doublets arises from the sulfur 2s peak. Only one type of Pt is detected in (b).

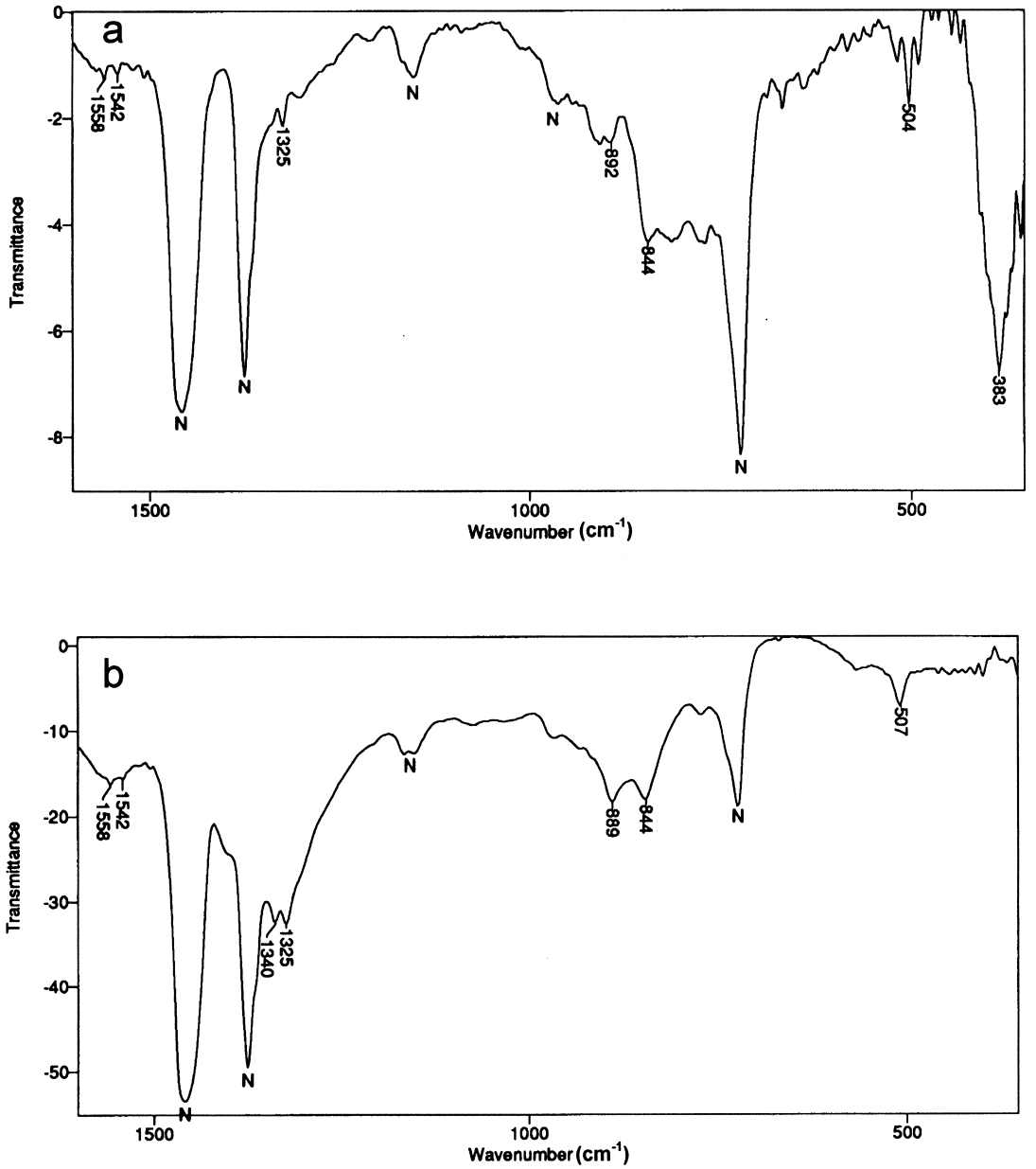

Fig. 4. Infrared spectra of (a) PtMoS[H_2O] and (b) [$Pt(NH_3)_4$]$C1_2H_2O$. The peaks arising from the N–H vibrations are indicated at 1558, 1542, 1340, 1325, 889, and 844 cm^{-1}. The peak at 383 cm^{-1} in (a) is indicative of the Mo–S stretching vibration for the cluster. (Peaks marked with an N arise from Nujol.)

indicated that the amount of MoS_2 in the treated materials was well below 1%. XPS spectra for the materials treated at 400–600°C indicated that surface Mo was largely in an intermediate oxidation state, with a binding energy too low to be MoS_2. After treatment at 800°C, MoS_2 was not detected by LRS, due to its reduction to Mo metal and H_2S (Fig. 6). XPS spectra for the 800°C treated material indicated virtually all of the surface Mo was in a reduced state consistent with Mo metal.

Weight losses were calculated for the treated samples (Fig. 7). During H_2 treatment, the solvent was removed and the ammine ligands associated with the Pt were driven off. The expected and observed weight losses (Table 3) were consistent. At higher temperatures (above 700 to 800°C), the weight loss corresponded to the formation of metallic species.

3.5. TPD/TPR results

TPD/TPR results were largely consistent with those from other characterization techniques (Fig. 8). During TPD of PtMoS[H_2O], two peaks arising from H_2O evolution were observed at about 120°C and 300°C (somewhat smaller). H_2O evolution ceased at about 400°C. The low temperature water peak was probably the result of desorption of loosely bound (physically adsorbed) H_2O. The

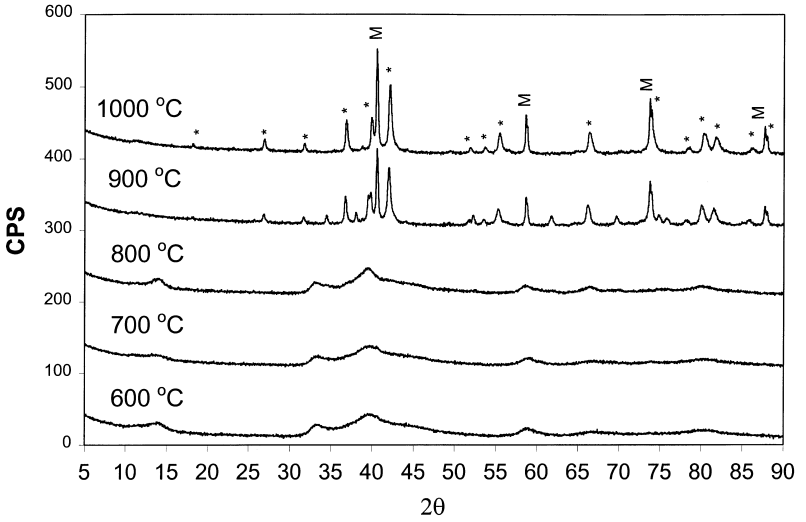

Fig. 5. X-ray powder diffraction of PtMoS prepared in pure MeOH and treated in flowing H_2 for 2 h at 600, 700, 800, 900, and 1000°C. Peaks labeled Mo and with an asterisk arise from Mo metal and the Pt–Mo alloy, respectively.

higher temperature peak was probably chemically bound (or chemisorbed) H_2O. H_2 evolution began at about 400°C and continued to 800°C. H_2O decomposition could lead to the formation of an intermediate oxide-sulfide species with a corresponding release of H_2.

During TPR, a large water peak and a H_2 uptake peak were observed at around 300°C and again at 475°C. H_2O production ended at about 900°C. H_2 uptake was still observable and actually began to increase at about 900°C as H_2S evolution occurred.

Temperatures for the phase changes indicated by TPR and XRD results did not directly correlate for two reasons. First, TPR was conducted in about 10% H_2 in N_2, while H_2 treatment experiments were performed in pure H_2. We have shown in previous TPR studies of LaMoS [22] that treatment in 10% H_2 increases the temperature at which H_2S evolution begins compared to treatment in pure H_2. Second, since TPR is a ramping experiment (while the treatment studies maintained the temperature for 2 h), any slow process in the chemical reactions likely increased the equivalent TPR temperature.

XPS spectra for the material after TPR (Fig. 9) indicated

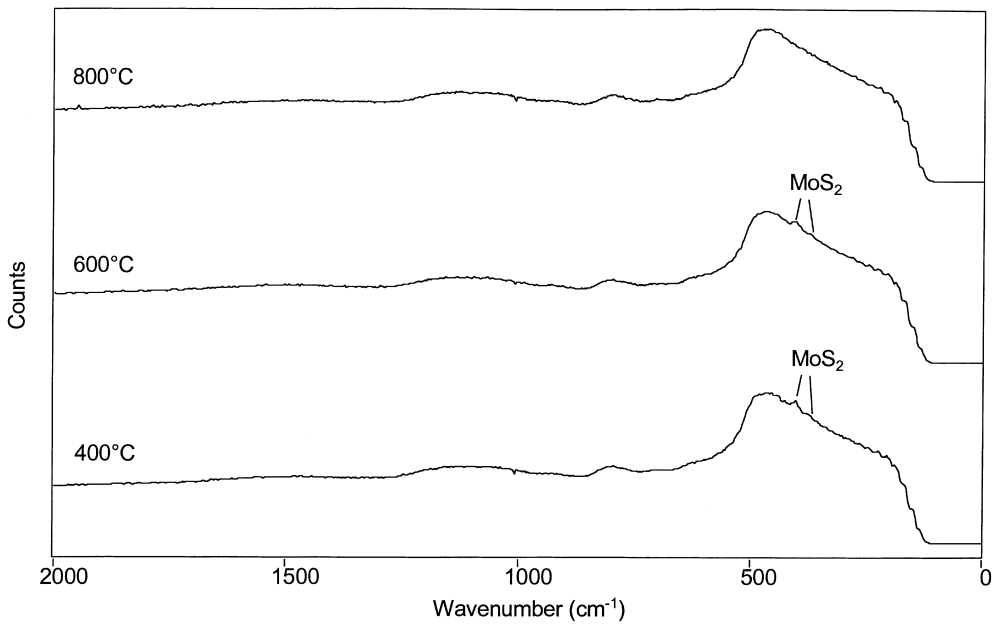

Fig. 6. Laser Raman spectra of PtMoS prepared in pure water and treated in pure, flowing H_2 for 4 h at 400, 600, and 800°C. The peak at 404 cm^{-1} is due to MoS_2.

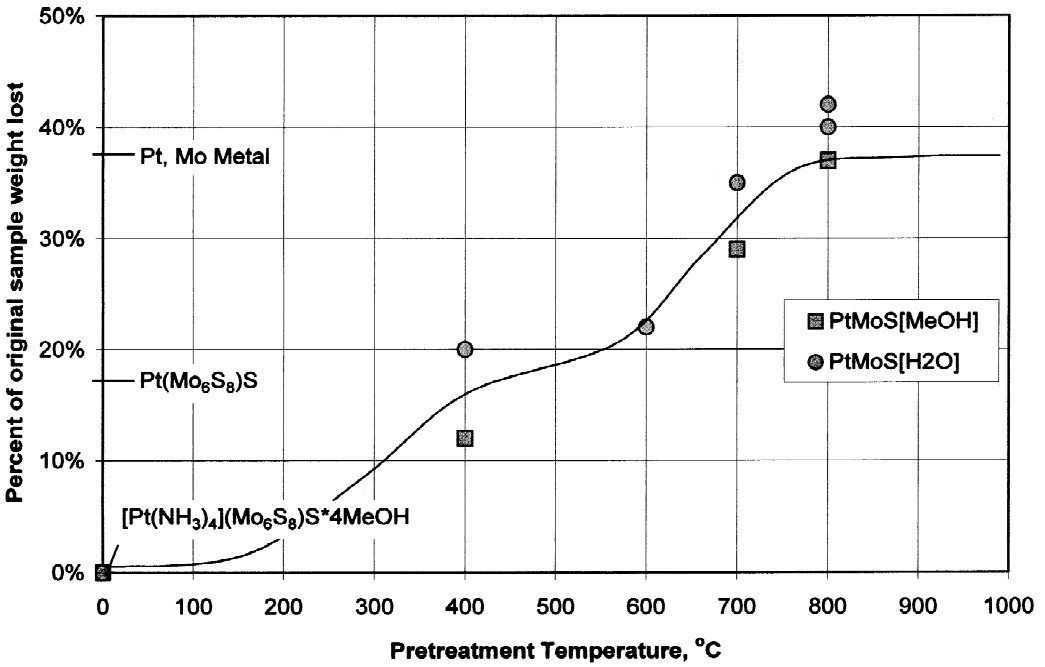

Fig. 7. Weight losses during H_2 treatment of PtMoS at various temperatures.

Table 3
Stoichiometry predicted percent weight losses for various final compositions, given the starting stoichiometry

	Starting material	
	$[Pt(NH_3)_4](Mo_6S_8)S{\cdot}4MeOH$	$[Pt(NH_3)_4](Mo_6S_8)S{\cdot}4H_2O$
$Pt(Mo_6S_8)S$	16	12
$Pt(Mo_6S_8)$	18	14
$PtMo_6$	39	36

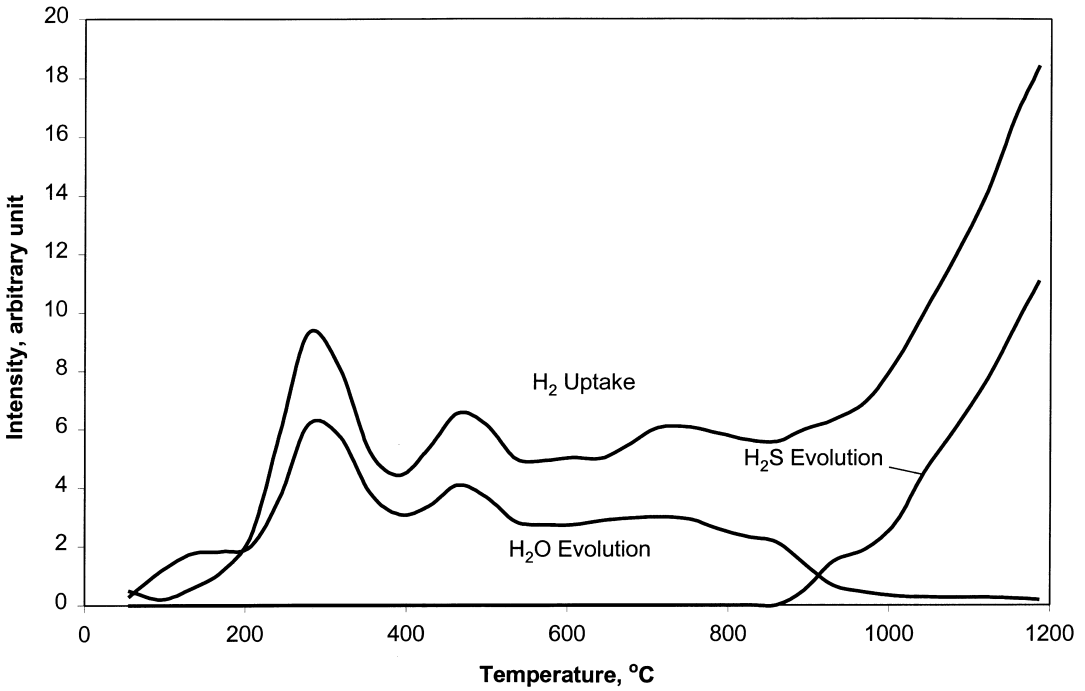

Fig. 8. Temperature-programmed reduction of PtMoS[5% H_2O] to 1200°C in flowing 10% H_2 in N_2. The PtMoS[5% H_2O] was prepared by ion-exchange in a 5% H_2O in MeOH solution.

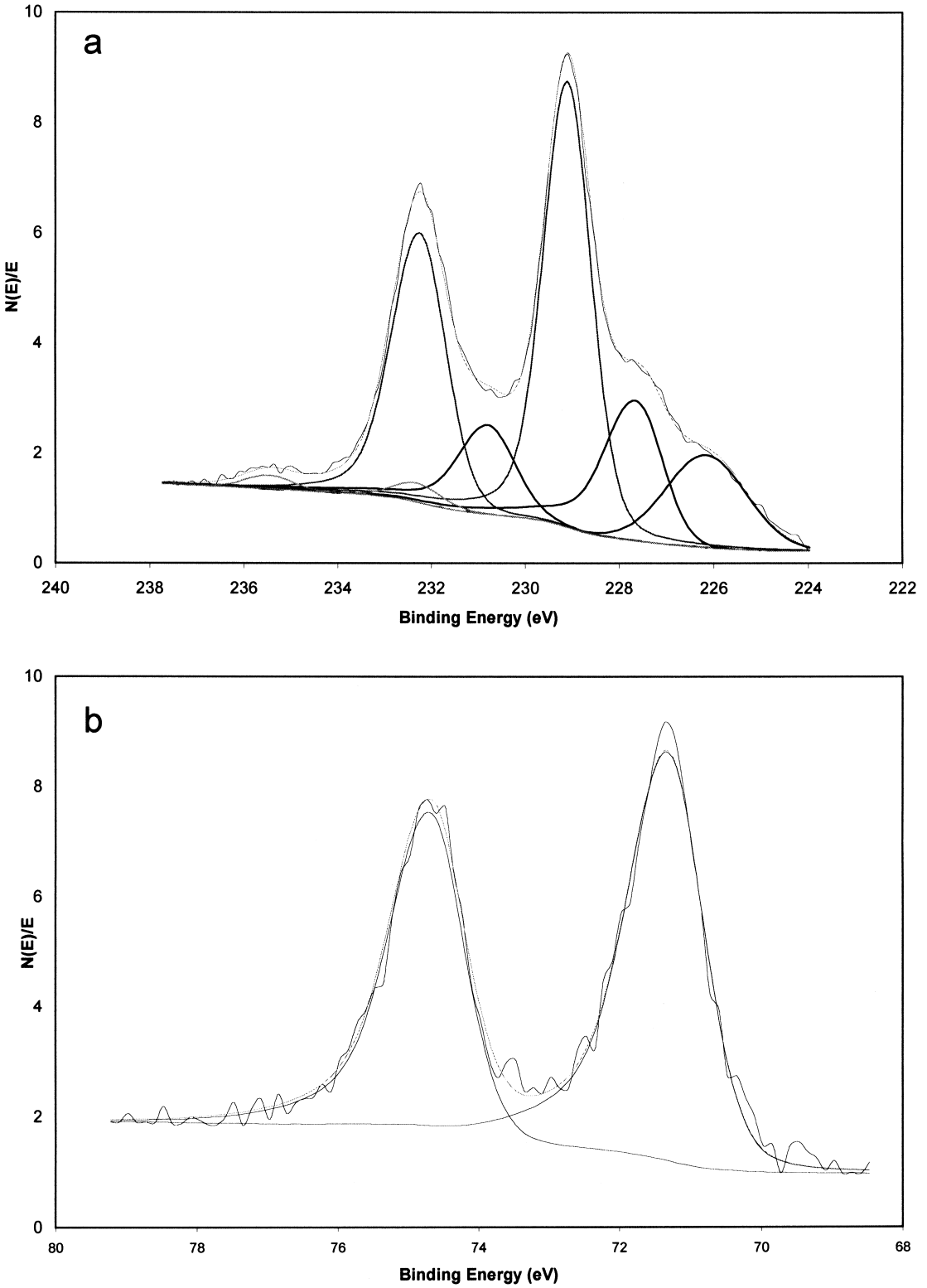

Fig. 9. X-ray photoelectron spectra for PtMoS[5% H_2O] prepared by ion-exchange in a 5% H_2O in MeOH solution, after TPR to 950°C in flowing 10% H_2 in N_2: (a) Mo 3d and (b) Pt 4f regions. Corrected Mo 3d binding energies consistent with the Mo_6S_8 cluster unit (228.1 eV) are detected in (a). The broad band observed at the lower binding energy side of the Mo 3d doublets arises from the sulfur 2s peak. Only one type of Pt is detected in (b).

Table 4
Thiophene HDS activities (400°C) after 10 h on stream

	Surface area (m^2/g) Before/after reaction	Thiophene conversion (mol%)	HDS rate ($mol/m^2s \times 10^8$)	% C_4 products			
				n-Butane	1-Butene	*trans*-2-Butene[e]	*cis*-2-Butene
$PtMoS[H_2O]$	21/6[d]	4.63	3.02	0.9	28.3	48.9	21.9
Reference materials							
SnMoS[a]	135/9	3.80	1.90	[f]	42.1	25.0	32.9
$LaMoS[LaCl_3$ prep$]$[b]	201/64	12.12	1.51	17.1	22.7	35.1	25.1
$LaMoS[La(NO_3)_3$ prep$]$[b]	200/54	2.62	0.32	5.5	41.0	32.4	21.1
Co–Mo–S[c]	10.83	0.89	3.36	1.5	36.4	41.1	21.0
MoS_2[c]	3.40	0.88	1.06	1.8	46.0	34.9	17.3

[a] Data from Ref. [20].
[b] Data from Ref. [19].
[c] Data from Refs. [9–12].
[d] Surface areas are reported before and after HDS, or after HDS where indicated as a single value.
[e] 1,3-Butadiene has identical retention time.
[f] Below detection limit.

that a new Mo species was present having an intermediate oxidation state and comprising the majority of the surface. The presence of a surface Mo oxide was consistent with previous work [22] and did not by itself indicate the destruction of the Mo_6S_8 cluster unit. Some surface MoO_3 was present also. XPS characterization for the as-prepared PtMoS showed a small chemical shift of about +0.3 eV for the Pt $4f_{7/2}$ peaks relative to Pt metal. However, after TPR, the chemical shift decreased to 0.1 eV; this was consistent with the reduction of Pt due to the loss of ammonia ligands, the presence of extra sulfur, and the reduction of the sample to Pt metal or a Pt–Mo alloy.

3.6. Thiophene HDS catalysis

HDS studies (Table 4) indicated that PtMoS activity was comparable to that for a 'CoMoS' reference material, based on rates normalized with respect to surface area. Mo_6S_8-based catalysts typically exhibit low selectivity for *n*-butane, but the PtMoS selectivity was particularly low. This is surprising since Pt metal is known to be an excellent hydrogenation catalyst. The PtMoS material had higher activity than any other amorphous ternary Mo_6S_8 material yet discovered, while retaining the remarkably low hydrogenation activity.

4. Conclusions

The amorphous sodium salt $Na_2(Mo_6S_8)S$ [NaMoS] has been shown to undergo cation exchange with $[Pt(NH_3)_4]^{2+}$ in H_2O, in 5% H_2O in MeOH, and in pure MeOH to produce the solvated derivative $[Pt(NH_3)_4]$ $(Mo_6S_8)S \cdot x(MeOH/H_2O)$ [PtMoS]. Analytical data show that the displacement of Na was nearly complete (>95%) upon reaction with one mole $[Pt(NH_3)_4]^{2+}$ per mole of NaMoS in these solvents. The high surface area of the starting material NaMoS was retained in the resulting PtMoS. FT-IR spectra of the latter indicated retention of the Mo_6S_8 cluster and the $[Pt(NH_3)_4]^{2+}$ cations. XPS revealed only one set of Mo 3d and Pt 4f bands with binding energies characteristic of these species in the as-prepared PtMoS. Laser Raman spectra confirmed the absence of MoS_2 in these preparations.

Conversion of PtMoS to the unknown crystalline Chevrel phase $PtMo_6S_8$ by hydrogen reduction at temperatures in the range of 400–800°C was attempted. While XRD showed weak reflections for a Chevrel phase in some samples, $NaMo_6S_8$ may have been formed due to incomplete removal of Na^+ during the ion-exchange process. Several samples of PtMoS showed formation of Pt, Mo, and perhaps a Pt–Mo alloy upon reduction at temperatures above 800°C. At lower temperatures, the H_2-treated material remained amorphous, and XPS indicated that the Mo_6S_8 cluster was retained below about 800°C. In the range of 400–500°C, the weight loss from PtMoS was in agreement with formation of $Pt(Mo_6S_8)S$. HDS studies indicated that these materials will likely be interesting catalysts for organosulfur reactions. In addition, the successful synthesis reported here for the first Mo_6S_8 material containing a platinum group element [in the anionic $(Mo_6S_8)S^{2-}$ network] indicates that other such derivatives containing Ru, Rh, Pd, Os, and Ir also might be prepared by related chemistry.

Acknowledgements

We thank Jim Anderegg for assistance in obtaining the XPS data. The microprobe analyses were completed by Dr. Alfred Kracher, Department of Geological and Atmospheric Sciences, at Iowa State University. This work was supported by the US Department of Energy, Office of Basic Energy Sciences, through Ames Laboratory operated by Iowa State University under Contract No. W-7405-Eng-82.

References

[1] R. Chevrel, M. Sergent, J.J. Prigent, Solid State Chem. 3 (1971) 515.
[2] R. Chevrel, M. Hirrien, M. Sergent, Polyhedron 5 (1986) 87.
[3] K. Yvon, in: Current Topics in Materials Science, Vol. 3, 1978, Chapter 2.
[4] J.D. Corbett, J. Solid State Chem. 39 (1981) 56.
[5] T. Hughbanks, R. Hoffmann, J. Am. Chem. Soc. 105 (1983) 1150.
[6] O.K. Anderson, W. Klose, H. Nohl, Phys. Rev. B 17 (1978) 1209.
[7] Ø. Fischer, Appl. Phys. 16 (1978) 1.
[8] Ø Fischer, M.B. Maple, in: Superconductivity in Ternary Compounds, Vol. I and II, Springer-Verlag, Berlin, 1982.
[9] K.F. McCarty, G.L. Schrader, Ind. Eng. Chem. Prod. Res. Dev. 23 (1984) 519.
[10] K.F. McCarty, J.W. Anderegg, G.L. Schrader, J. Catal. 93 (1985) 375.
[11] M.E. Eckman, J.W. Anderegg, G.L. Schrader, J. Catal. 117 (1989) 246.
[12] I.M. Schewe-Miller, K.F. Koo, M. Columbia, F. Li, G.L. Schrader, Chem. Mater. 6 (1994) 2327.
[13] S.A. Kareem, R. Miranda, J. Molec. Catal. 53 (1989) 275.
[14] J.M. Tarascon, J.V. Waszczak, G.W. Hull Jr., F.J. DiSalvo, L.D. Blitzer, Solid State Commun. 47 (1983) 973.
[15] J.M. Tarascon, F.J. DiSalvo, D.W. Murphy, G. Hull, J.V. Waszczak, Phys. Rev. B 29 (1984) 172.
[16] R. Schollhorn, M. Kümpers, J.O. Besenhard, Mat. Res. Bull. 12 (1977) 781.
[17] R. Chevrel, M. Sergent, J. Pringent, Mat. Res. Bull. 9 (1974) 1487.
[18] R.E. McCarley, S.J. Hilsenbeck, X. Xie, J. Solid State Chem. 117 (1995) 269.
[19] W.T. Elwell, W.F. Wood, in: Analytical Chemistry of Molybdenum and Tungsten, Pergamon Press, New York, 1971, p. 41.
[20] S.J. Hilsenbeck, R.E. McCarley, R.K. Thompson, L.C. Flanagan, G.L. Schrader, J. Molec. Catal. A: Chemical 122 (1997) 13.
[21] S.J. Hilsenbeck, R.E. McCarley, A.I. Goldman, G.L. Schrader, Chem Mater. 10 (1998) 125.
[22] R.K. Thompson, S.J. Hilsenbeck, T.J. Paskach, R.E. McCarley, G.L. Schrader, J. Molec. Catal. A: Chemical (in press).
[23] S.J. Hilsenbeck, Unpublished data.